N95-14562

Pool and Flow Boiling in Variable and Microgravity

8P

Herman Merte, Jr.
Professor of Mechanical Engineering
The University of Michigan
Ann Arbor, Michigan

INTRODUCTION

As is well known, boiling is an effective mode of heat transfer in that high heat flux levels are possible with relatively small temperature differences. Its optimal application requires that the process be adequately understood. A measure of the understanding of any physical event lies in the ability to predict its behavior in terms of the relevant parameters. Despite many years of research the predictability of boiling is currently possible only for quite specialized circumstances, e.g., the critical heat flux and film boiling for the pool boiling case, and then only with special geometries.

Variable gravity down to microgravity provides the opportunity to test this understanding, but possibly more important, by changing the dimensional and time scales involved permits more detailed observations of elements involved in the boiling process, and perhaps discloses phenomena heretofore unknown.

The focus here is on nucleate boiling although, as will be demonstrated below, under certain circumstances in microgravity it can take place concurrently with the dryout process. In the presence of earth gravity or forced convection effects, the latter process is usually referred to as film boiling. However, no vapor film as such forms with pool boiling in microgravity, only dryout. Initial results are presented here for pool boiling in microgravity, and were made possible at such an early date by the availability of the Get-Away-Specials (GAS).

Also presented here are some results of ground testing of a flow loop for the study of low velocity boiling, eventually to take place also in microgravity. In the interim, variable buoyancy normal to the heater surface is achieved by rotation of the entire loop relative to earth gravity. Of course, this is at the expense of varying the buoyancy parallel to the heater surface. Two questions which must be resolved early in the study of flow boiling in microgravity are (1) the lower limits of liquid flow velocity where buoyancy effects become significant to the boiling process (2) the effect of lower liquid flow velocities on the Critical Heat Flux when buoyancy is removed. Results of initial efforts in these directions are presented, albeit restricted currently to the ever present earth gravity.

POOL BOILING

Before a nucleate pool boiling system can attain the steady periodic behavior normally observed in a gravity field, where buoyancy is the predominant vapor removal mechanism, the process must pass through a transient phase. Where the buoyancy is drastically reduced, as in microgravity, the process is anticipated to be inherently transient unless some special circumstances can be provided to maintain a subcooled bulk liquid domain. Absent this, the elements of transient boiling possible are:

(a) Conduction
(b) Onset of natural convection
(c) Nucleation
(d) Vapor bubble growth/collapse
(e) Departure
(f) Motion following departure

In the transient pool boiling experiments conducted in the microgravity of space in the GAS on the shuttle STS-47, only elements (a), (c) and (d) were present and are considered here. The heater surface used is rectangular in shape, 1.91 cm by 3.81 cm (0.75 × 1.5 inches), consisting of a 400 Angstrom thick semi-transparent gold film sputtered on a quartz substrate, and serves simultaneously as a heater and a resistance thermometer. Viewing is provided simultaneously from the underside and side of the heater surface. Degassed R-113 with a normal boiling point of 47.2°C (117°F) was used as the working fluid. The subcooling level was controlled by varying the system

pressure, which was maintained constant to within ± 690 N/m^2 (± 0.1 psi) during any particular test. The experimental technique followed is described in ref. (1).

Measurement of the mean heater surface resistance, and hence temperature, was obtained at 10 Hz, and permitted the computation of heat transfer by conduction to the substrate, and to the fluid, from which a mean heat transfer coefficient was determined.

Figures 1 and 2 present the measured heater surface temperature and heat transfer coefficients for 2 of the 9 tests conducted. It is noted that a quasi-steady process exists for this subcooled case during the some 75 seconds of active boiling, although a tendency toward a decrease exists at the end. The 9 tests which constitute the matrix of test conditions are shown in Table 1. The behavior at earth gravity obtained following the space flight are compared with that in microgravity. Boiling in microgravity under these conditions, with a relatively large flat heater surface, appears quite unstable.

The heater surface superheat at the moment of nucleation are plotted in Fig. 3 as a function of heat flux with subcooling as a parameter for the identical system in microgravity, and post-and pre-flight. A rather anomalous behavior is noted in that the heater surface superheat required to nucleate the fluid is a maximum at the intermediate heat flux level. A similar behavior occurred with a different system in the STS-57. The maximum is also noted when the system is operated inverted in earth gravity. In ground based testing reported in ref. (2), nucleation at a/g = -1 occurred at heater surface superheats of approximately 10°C at heat flux levels varying from 50 w/cm^2 at a subcooling of 11°C to 22 w/cm^2 with a saturated liquid. These are consistent with extrapolations to the right in Fig. 3. Future space experiments are proposed to explore heat flux levels down to 0.5 w/cm^2, which would extrapolate Fig. 3 to the left.

It is observed in Fig. 2, which applies for the lowest level of heat flux and virtually saturated liquid, that a correspondence exists between decreases in the mean surface temperature and increases in the mean heat transfer coefficient. This is not unexpected, since the latter is determined from the former. Upon viewing the motion pictures taken through the heating surface from the underside it was noted also that a decrease in the mean heat transfer coefficient corresponded to a distinct increase in the heater surface dryout area. Provision was made for the measurement of the fractional dry area of each frame of the 16 mm film, and examples are given in Fig. 4 for Run No. 9 in Fig. 2. Fig. 4a is for the region of 61.5 — 67.5 seconds, in which the surface is rewetting, while Fig. 4b is for the region of 80.5 — 85.5 seconds, in which the surface is drying out again. These behaviors are apparently random, and are the subject for further proposed microgravity experiments at lower levels of heat flux and higher levels of bulk liquid subcooling.

If the assumption is made that the heat transfer to the fluid in the dry portion of the heater surface can be neglected, and that the heat transfer coefficient over the remaining wetted portion of the heater surface is approximately uniform, then this latter quantity can be determined by dividing the overall mean heat transfer coefficient by the fractional wetted area. These results are also plotted in Figs. 4a and 4b, and show that the microgravity boiling heat transfer coefficients are virtually the same during the rewetting and dryout phases, 1250 and 1200 w/cm^{2}C, respectively. Each data point in Fig. 4 corresponds to a single frame, taken at 10 pps, and the oscillations are a reality in the physical process. The rather large excursions in the boiling heat transfer coefficients early in Fig. 4a and late in Fig. 4b are a consequence of the inherent relatively large uncertainty in measurement of the fractional wet area at low levels of wetting, and should be disregarded.

FLOW BOILING

A schematic of the low velocity forced convection boiling loop for proposed studies with R-113 in microgravity is shown in Fig. 5, with a more detailed view of the test section in Fig. 6. Velocities can be varied from 0.5 cm/s to 32 cm/s by pump speed control combined with changes in test section height, from 2.54 cm (1 inch) to 0.318 cm (0.125 inch). The use of a flow loop permits the study of boiling under steady conditions as well as under transients, as in the prior described pool boiling studies, and thus can accommodate the use of more massive metallic surfaces which, while more representative of engineering surfaces, also introduce complications associated with heat capacity effects. The flow loop proper occupies a volume of about 1.22 × .61 × .46 m (48 × 24 × 18 inches).

Although up to 6 heater surfaces can be accommodated simultaneously, a maximum of 3 is anticipated, with the remaining ports used for visualization. In addition to the gold film on quartz substrate heaters described previously, two flat metallic substrate heaters are used, with the same dimensions as the gold film heaters, but with maximum heat flux capabilities to 15 w/cm^2 and 75 w/cm^2. The latter heater is used for Critical Heat Flux studies with R-113, and has a larger uncertainty in the heat flux measurement at the lower levels of heat flux, below about 20 w/cm^2. System pressure, fluid temperature at the test section inlet, and flow rate controls are completely automated. More details on the flow loop and heater surfaces are available in refs. (3) and (4).

Fig. 7 is a sample result from ref. (5), showing how buoyancy influences the boiling heat transfer behavior at a low level of velocity of 4.1 cm/s. In single phase mixed convection heat transfer both buoyancy and imposed bulk liquid flow provide the mechanisms for fluid motion, where the relative significance of these is characterized by the Richardson number. For dealing with the combined effects of buoyancy and imposed bulk liquid flow with boiling, a "two-phase Richardson number" is developed in ref. (5) and (6), and is shown as the lower curve in Fig. 8 as a function of N_d, the product of the Weber and square of the Froude numbers. Also included as the upper curve in Fig. 8 is the square of the velocity ratio of Siegel (ref. 7), used to describe the rise velocity relative to a fluid flowing vertically. Tentative bounds are included in Fig. 8 for inertial and buoyant dominated domains, based as yet on limited experimental data. It is anticipated that experimentation proposed for parabolic flights in aircraft will provide additional data for bracketing more closely the relative influences of buoyancy and inertial effects.

Figs. 9 and 10, from ref. (4), show measurements of the Critical Heat Flux (CHF) at relatively low and high velocities, respectively, with R-113 at various orientations of the flat heater surface relative to the buoyancy vector. The angle $\theta = 0$ applies to the horizontal upward facing orientation. The CHF is normalized relative to a pool boiling correlation of ref. (1), q_{co}, which includes the influence of bulk liquid subcooling. The curves labeled "model" in Figs. 9 and 10 are for pool boiling modified by multiplying by the square root of θ over the interval of 90 to 270 deg., and arise from equating buoyancy and drag forces in the inverted positions where the vapor bubbles are held against the heater surface as they slide. The model is described in ref. (4).

The onset of forced convection effects become quite distinctive between Figs. 9 and 10, and it can be anticipated that the CHF will become independent of θ at sufficiently large velocities. Plans are underway to increase the maximum velocity attainable to about 60 cm/s. It can also be anticipated that the behavior of the CHF will take on quite another character in microgravity, where buoyancy effects become totally negligible. The only forces remaining then are momentum (or inertia) of the bulk liquid flow and surface tension, both liquid-vapor and liquid-vapor-solid. These can be expected to influence not only the CHF (or dryout - more likely), but the departure sizes of the vapor bubbles as well.

REFERENCES

1. Ervin, J. S., Merte, H., Jr., Keller, R. B., Kirk, K., "Transient Pool Boiling in Microgravity," Int. J. Heat Mass Trans., 35, March, 1992, pp. 659-674.
2. Ervin, J. S., Merte, H. , Jr., "A Fundamental Study of Nucleate Pool Boiling under Microgravity," Final Report to NASA Lewis Research Center on NASA Grant NAG3-663, Report No. UM-MEAM-91-08. August, 1991.
3. Kirk, K. M., Merte, H., Jr., Keller, R. B., "Low Velocity Nucleate Flow boiling at Various Orientations," ASME Symposium-Fluid Mechanics Phenomena in Microgravity, Ed. by D. A. Siginer and M. M. Weislogal, AMD - Vol. 154/FED - Vol. 142. 1992.
4. Brusstar, M. J., Merte, H., Jr., "Effects of Buoyancy on the Critical Heat Flux in Forced Convection," AIAA J. Thermophysics and Heat Transfer, 8, April - June, 1994, pp. 322-328.
5. Kirk, K. M., Merte, H. Jr., "A Study of the Relative Effects of Buoyancy and Liquid Momentum in Forced Convection Nucleate Boiling," Final Report to NASA Lewis Research Center on NASA Grant NAG3-1310, Report No. UM-MEAM-92-06. November, 1992.
6. Kirk, K. M., Merte, H., Jr., "A Mixed Natural/Forced Convection Nucleate Boiling Heat Transfer Criteria," Proceedings of 10th International heat Transfer Conference, Aug. 14-18, 1994, Brighton, U.K.
7. Siegel, R., "Effect of Reduced Gravity on Heat Transfer," Advances in Heat Transfer, eds. James P. Hartnett and Thomas F. Irvine, Vol. 4, pp. 200-205.
8. Ivey, H. J., Morris, D. J., "On the Relevance of the Vapour-Liquid Exchange Mechanism for Subcooled Boiling Heat Transfer at High Pressure," UKAEA, AEEW-R-137, 1962.

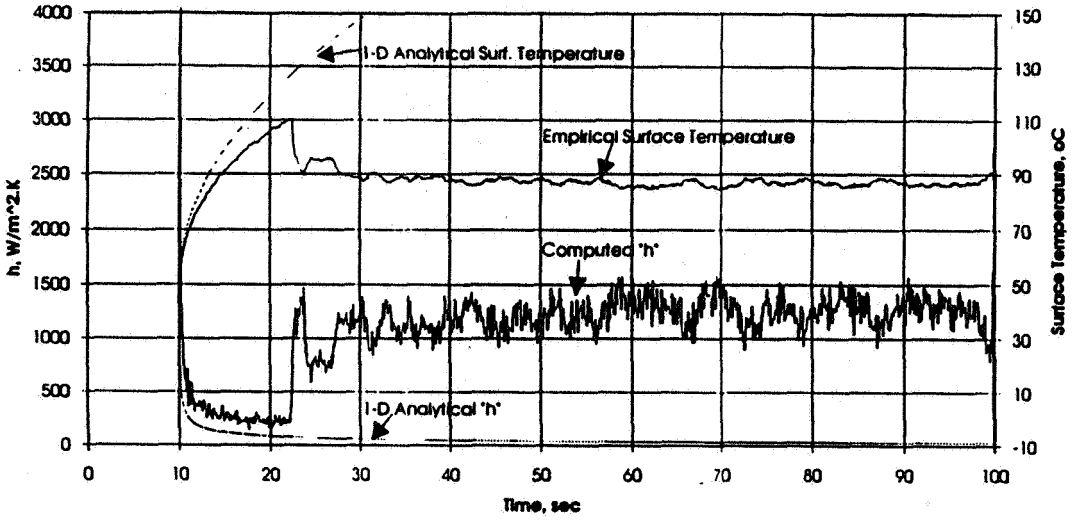

Figure 1. Mean heater surface temperature and heat transfer coefficient. R-113. PBE Prototype. STS-47. Run No. 2. q''_T = 3.6 w/cm^2. ΔT_{sub} = 11.9°C. T_{sat} = 61.1°C.

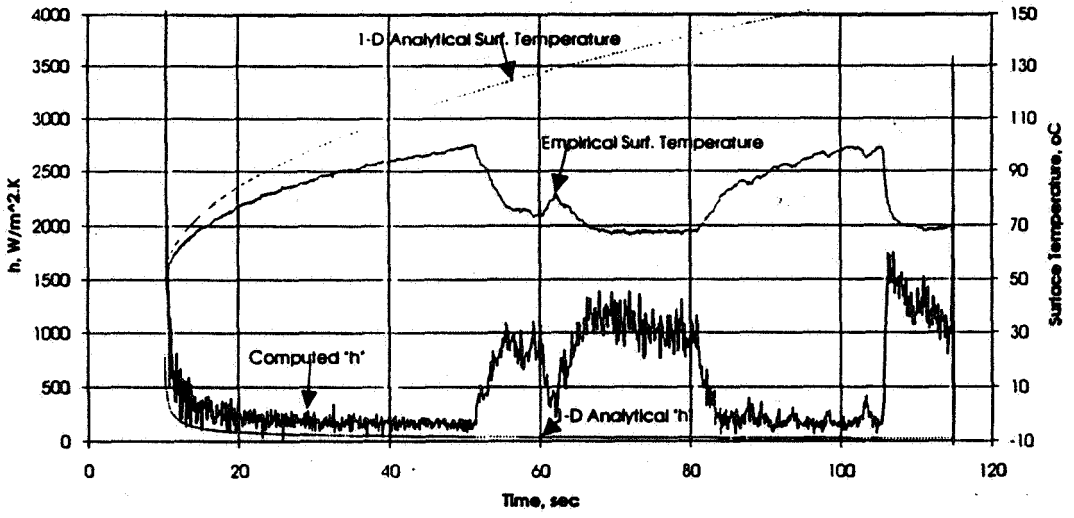

Figure 2. Mean heater surface temperature and heat transfer coefficient. R-113. PBE Prototype. STS-47. Run No. 9. q''_T = 1.8 w/cm^2. ΔT_{sub} = 0.2°C. T_{sat} = 49.4°C.

Run No.	q" w/cm² Approx.	Δ T_{sub} °C Approx.	h w/m²K a/g = +1 Post Flight 11/4/92	h w/m²K a/g ≅ 10^{-5} STS-47
1	7.0	10.7	2500 Nucleate Boiling	700 Dry Out
2	3.6	11.5	1300 Nucleate Boiling	1250** Steady State + Oscillating
3	1.8	11.0	450 (350)* Non-Boiling Convection	1100 → 600 Steady State → Dry Out
4	7.0	2.7	2300 Nucleate Boiling	200 Dry Out
5	3.6	2.8	550 (430)* Non-Boiling Convection	400 → 200 Increased Dry Out
6	1.8	2.8	550 (350)* Non-Boiling Convection	1150 Steady State + Oscillating (Rewet)
7	7.0	0.6	2300 Nucleate Boiling	200 Dry Out
8	3.5	0.4	600 (400)* Non-Boiling Convection	300 → 200 Increased Dry Out
9	1.8	0.2	500 (350)* Non-Boiling Convection	1100 → 200** Steady State + Dry Out & Rewet

* Computed from natural convection correlation: $Nu = 0.15 \times Ra^{1/3}$
** Detailed results following.

Table 1. Comparison of measured mean heat transfer coefficients for PBE Prototype between a/g = +1 and STS-47 space flight.

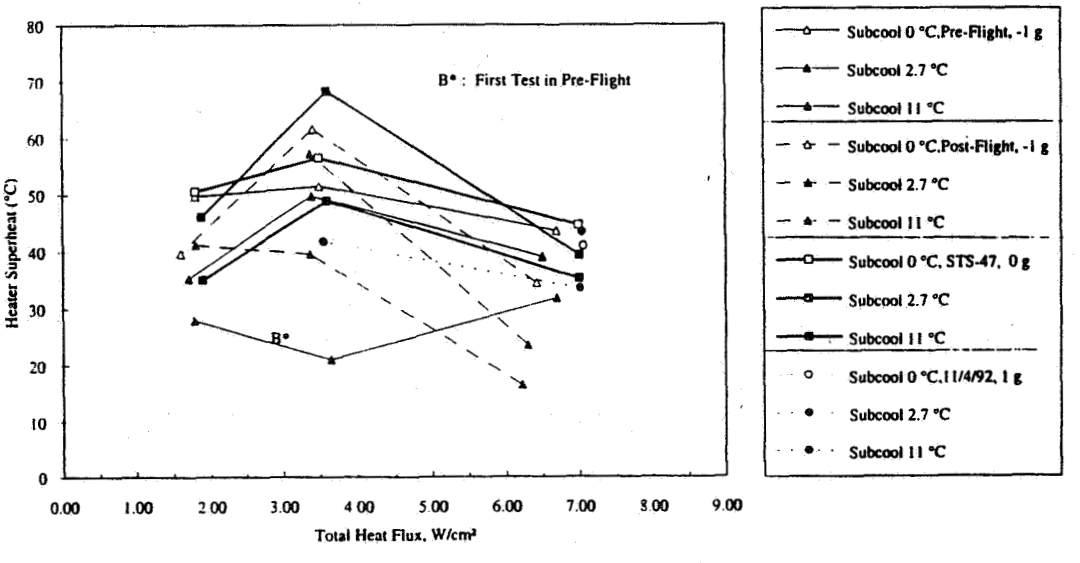

Figure 3. Heater surface superheat at nucleation for PBE Prototype System for a/g = ± 1 and STS-47 space flight.

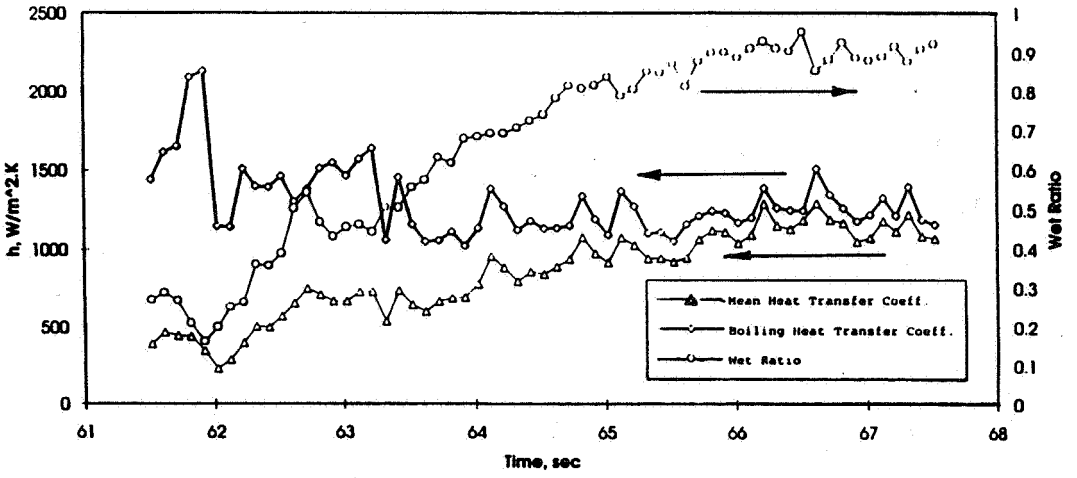

a. Rewetting portion of Figure 2. 61.5 — 67.5 sec.

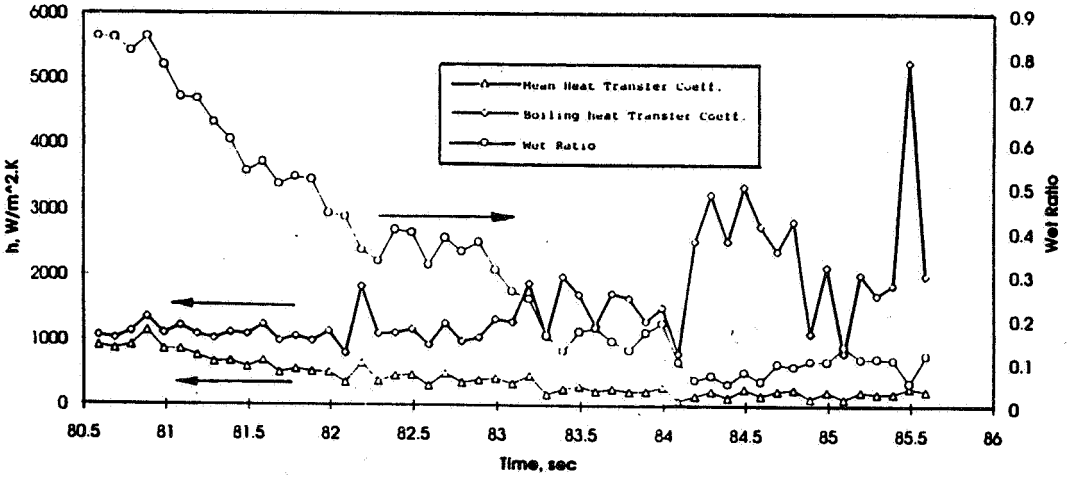

b. Dryout portion of Figure 2. 80.5 — 85.5 sec.

Figure 4. Fractional wetted area — nucleate boiling heat transfer coefficient — mean heat transfer coefficient with rewetting and dryout. PBE Prototype. STS-47. Run No. 9. $q''_T = 1.8$ w/cm^2. $\Delta T_{sub} = 0.2$°C. $T_{sat} = 49.4$°C.

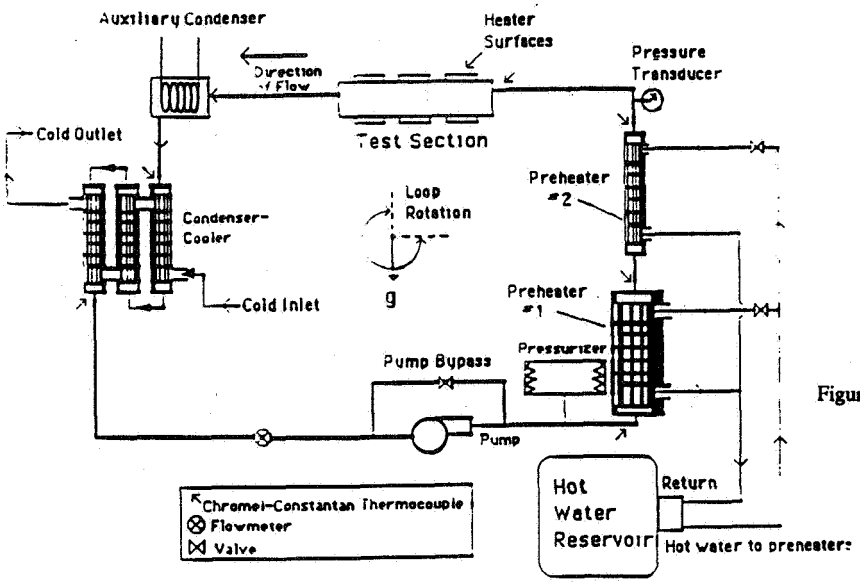

Figure 5. Low velocity boiling loop for variable orientation and low gravity.

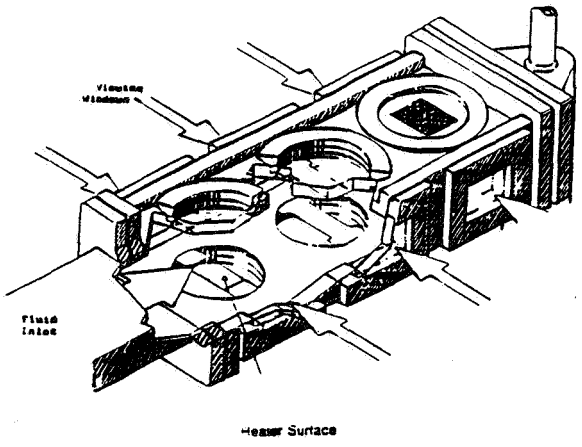

Figure 6. Test section. Flow area = 10.80 cm (4.25 in.) wide x 0.318, 1.27 or 2.54 cm (0.125, 0.50 or 1.0 in.) high.

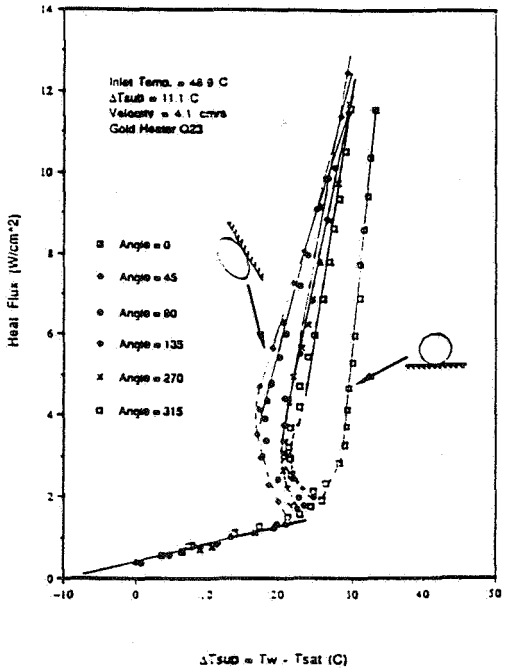

Figure 7. Heat flux vs heater surface superheat at various orientations. Test Section inlet temperature = 48.9°C. ΔT_{sub} = 11.1°C. Velocity = 4.1 cm/sec. Gold film heater on quartz.

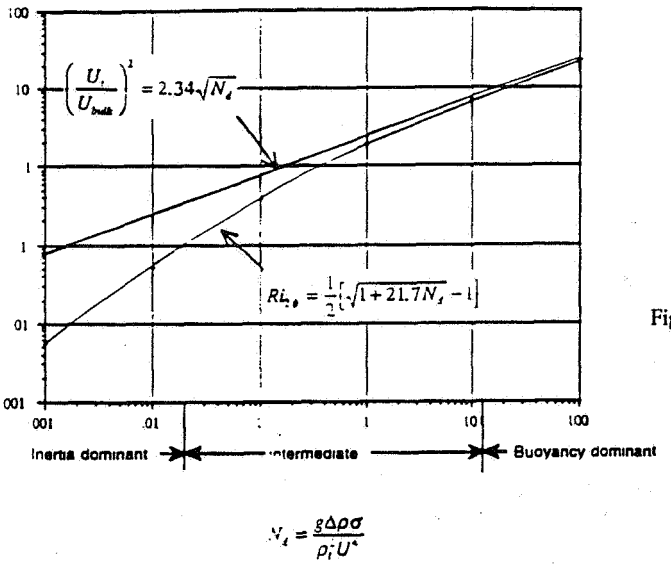

Figure 8. Flow effects relative to buoyancy with boiling.

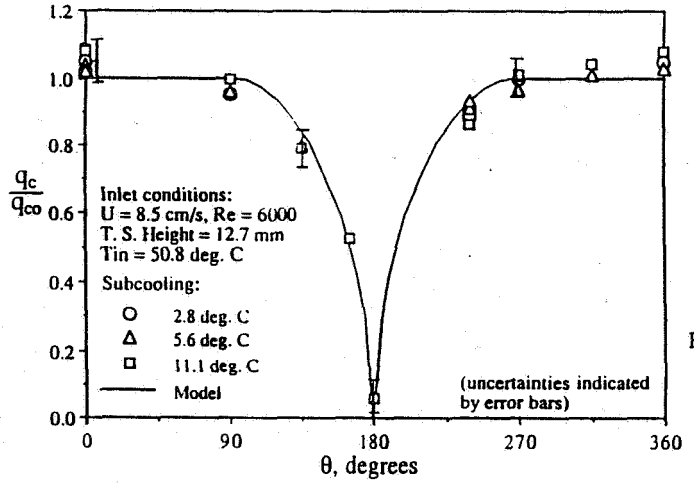

Figure 9. Critical Heat Flux at various orientations with low velocity (8.5 cm/s). R-113.

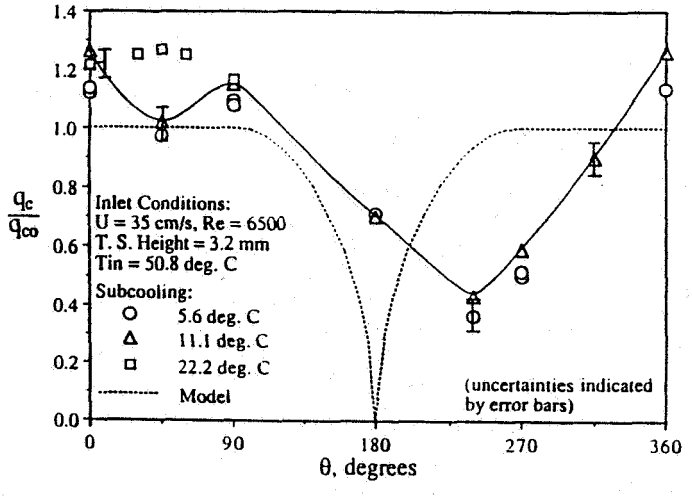

Figure 10. Critical Heat Flux at Various orientations with relatively high velocity. (35 cm/s). R-113).